

# Lecture 21. Wind Lidar (3)

## Direct Detection Doppler Lidar

- ❑ Overview of Direct Detection Doppler Lidar (DDL)
- ❑ Resonance fluorescence DDL
- ❑ Fringe imaging DDL
- ❑ Scanning FPI DDL
- ❑ FPI edge-filter DDL
- ❑ Absorption line edge-filter DDL
- ❑ Comparison of various DDL techniques

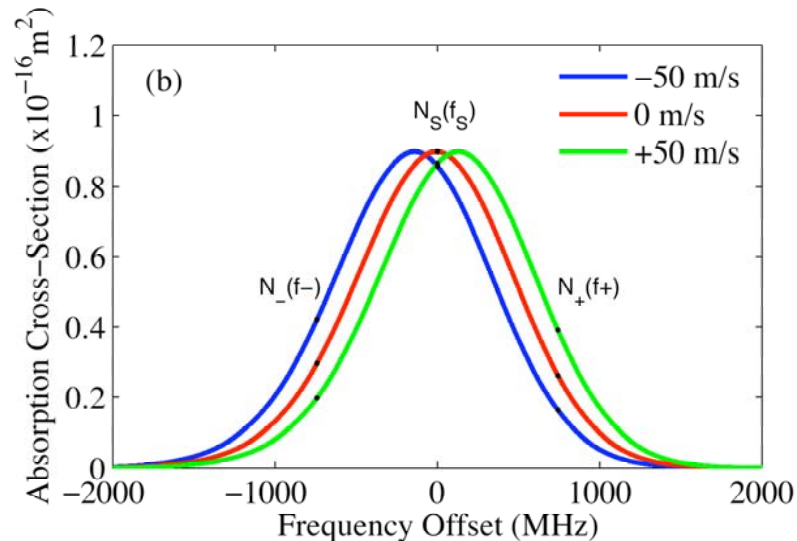
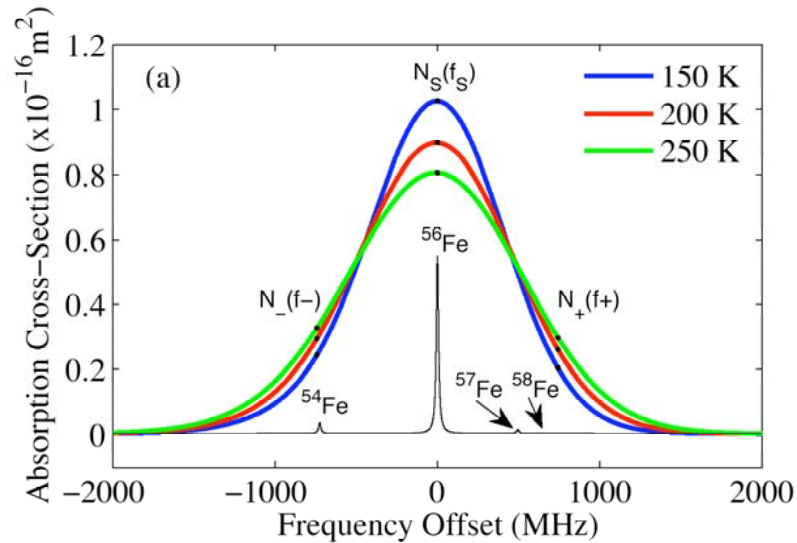
# Direct Detection Doppler Wind

- ❑ Direct detection Doppler lidars (DDL) convert the Doppler frequency shift to the change of intensity, or intensity ratio, or intensity spatial distribution.
- ❑ One of the key components for non-resonance DDL is the optical frequency discriminator or frequency analyzer, usually implemented in the lidar receiver. Current available **optical frequency discriminators** include
  - (1) Fringe imaging with optical interferometer (Fabry-Perot or Fizeau or Mach-Zahnder)
  - (2) Scanning Fabry-Perot interferometer (FPI)
  - (3) Interferometer edge-filter: the edge of a transmission fringe of an optical interferometer (e.g., Fabry-Perot etalon),
  - (4) Absorption line edge-filter: (e.g., iodine I<sub>2</sub> absorption lines)
- ❑ A major difference between resonance DDL and non-resonance DDL lies in where the frequency discriminator is - in the atmosphere or in the receiver chain! Because the Na, K, or Fe absorption lines are in the atmosphere, the lidar receiver is allowed to be broadband, rather than the narrowband employed in the non-resonance DDL.

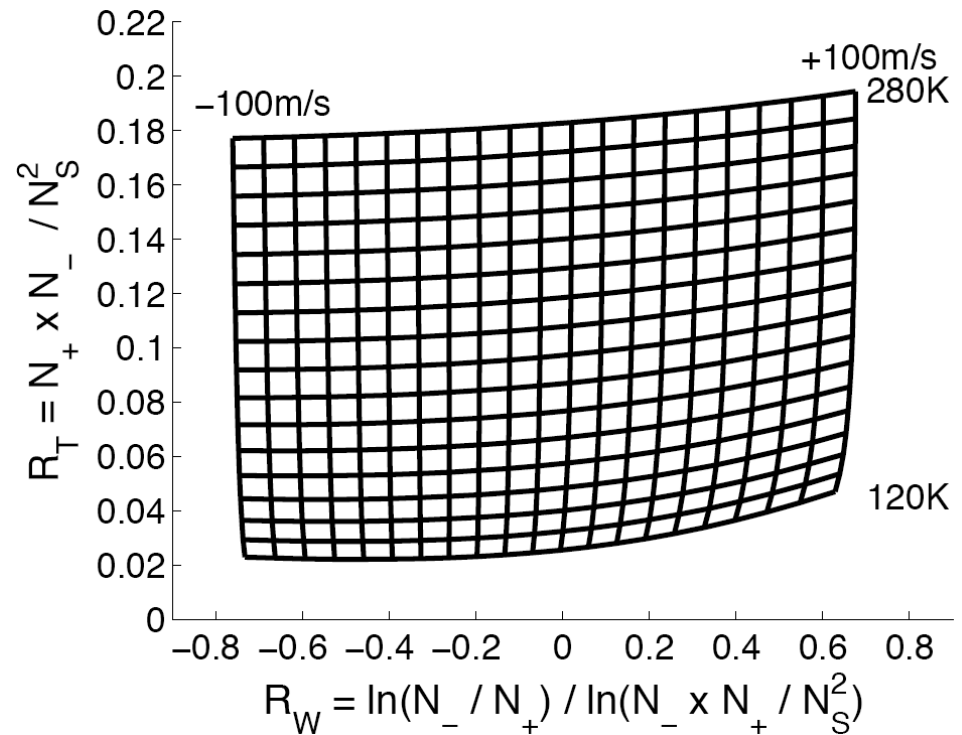
# Consideration for DDL

- ❑ Precision requirement: for  $\delta V = 1$  m/s velocity precision, the freq measurement precision required for the optical freq analyzer in a DDL is  $\delta \nu = 2(\delta V)/\lambda = 5.6$  MHz for 355 nm.
- ❑ Accuracy requirement: accuracy should surpass the precision level. This is usually achieved by monitoring the transmitted laser pulse signal or alternatively measuring the backscatter signal from a stationary or very low velocity target or lock the laser and the filter transmission to each other.
- ❑ Calibration or accuracy is a main problem for non-resonance DDL, because the burden is on the receiver chain which is variable through time or surrounding conditions, especially in FPI case.
- ❑ On the other hand, resonance fluorescence Doppler lidars put the discriminator to the atomic absorption lines, which do not change with time. Their receivers can be much simpler.

# Resonance Fluorescence DDL

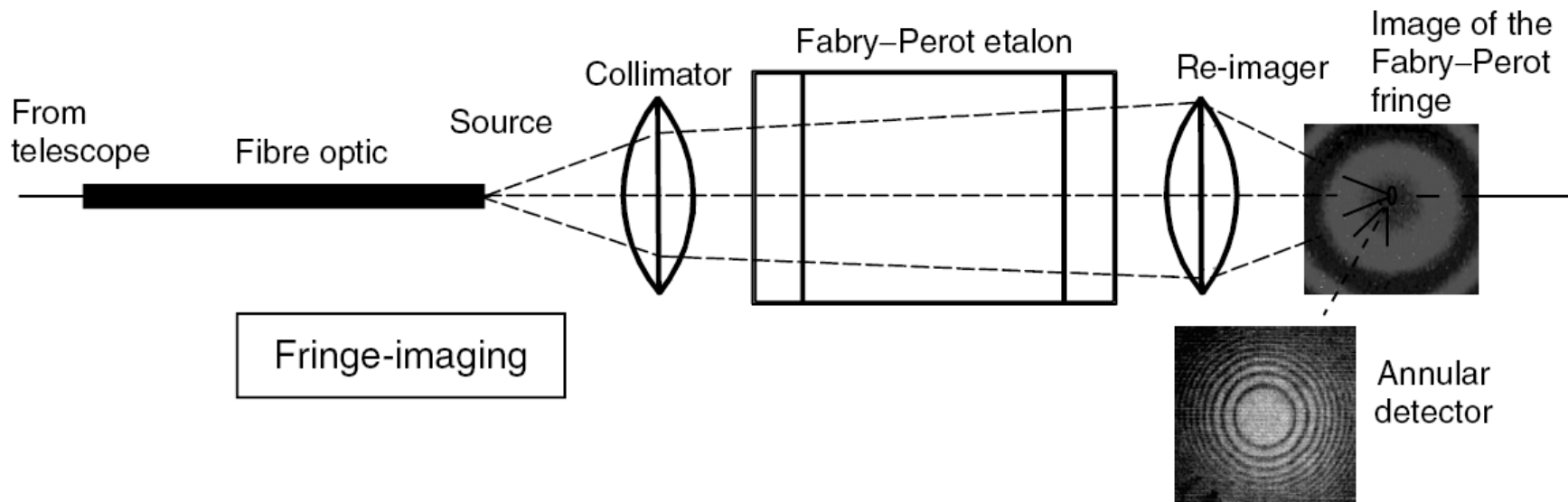


## Fe Doppler Lidar



Atomic Fe absorption lines undergo Doppler frequency shift & broadening, so acting as an frequency analyzer/discriminator

# Freq Analyzer: Fringe-Imaging

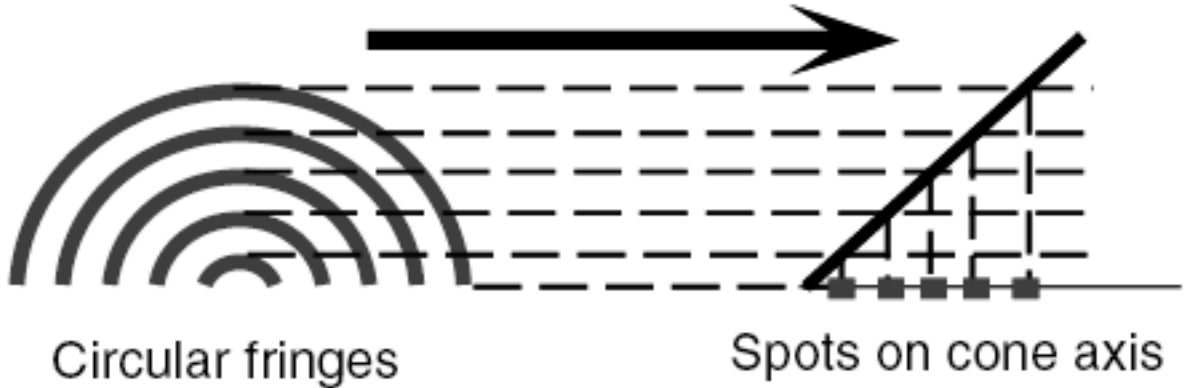
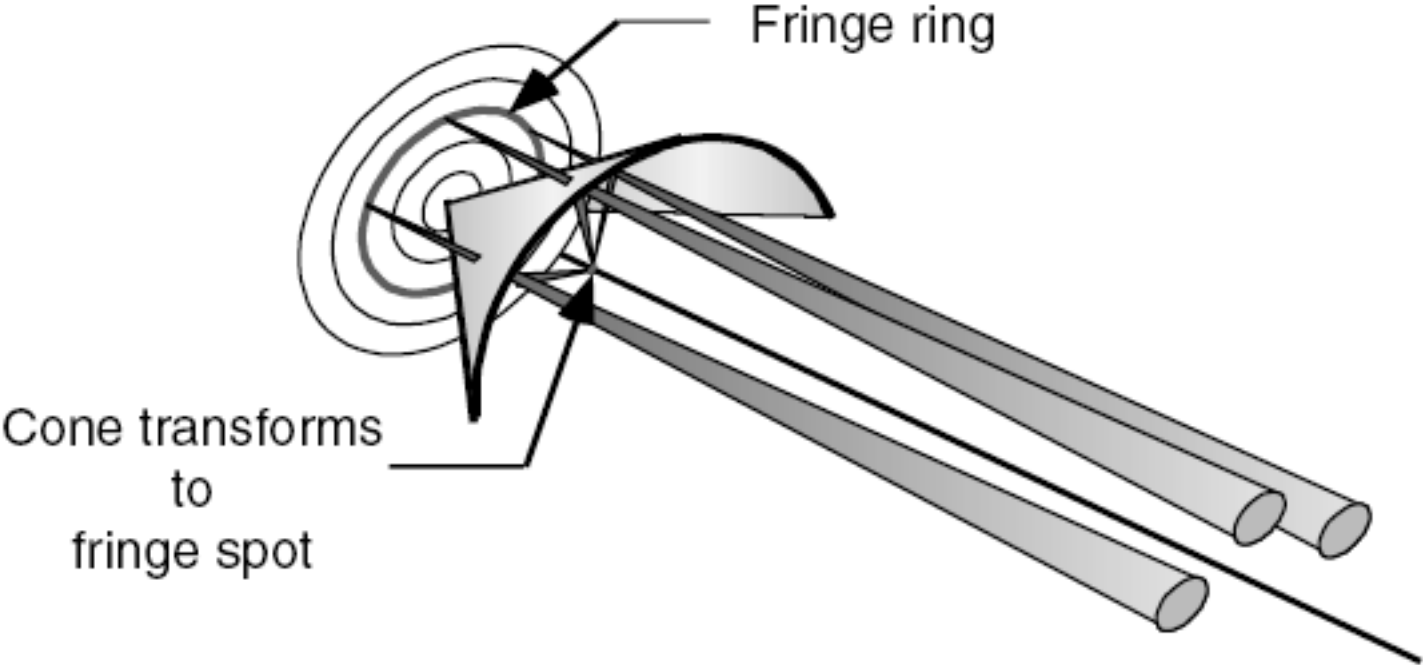


- ❑ The basic concept of fringe-imaging discriminator is to utilize a high-resolution interferometer to produce a spatial irradiance distribution, which is representative of the receiver-plane signal spectrum.
- ❑ In principle, fringe imaging can measure both wind (from frequency shift) and temperature (from fringe width).
- ❑ Similar to passive F-P Interferometer, the diameter of the concentric rings can be used to determine the frequency shift.

# Detectors for Fringe Imaging DDL

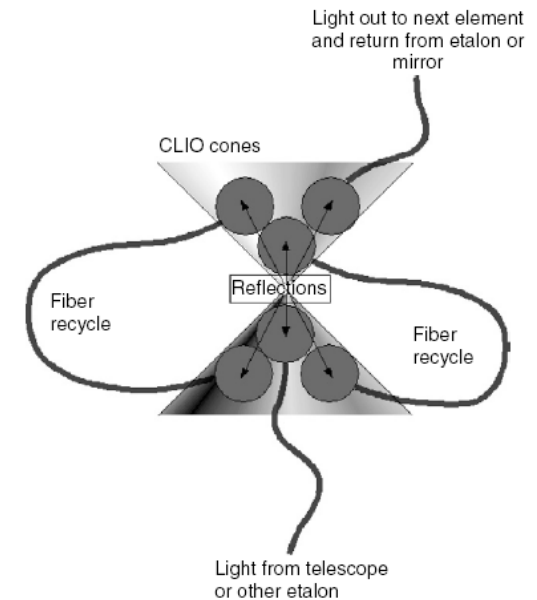
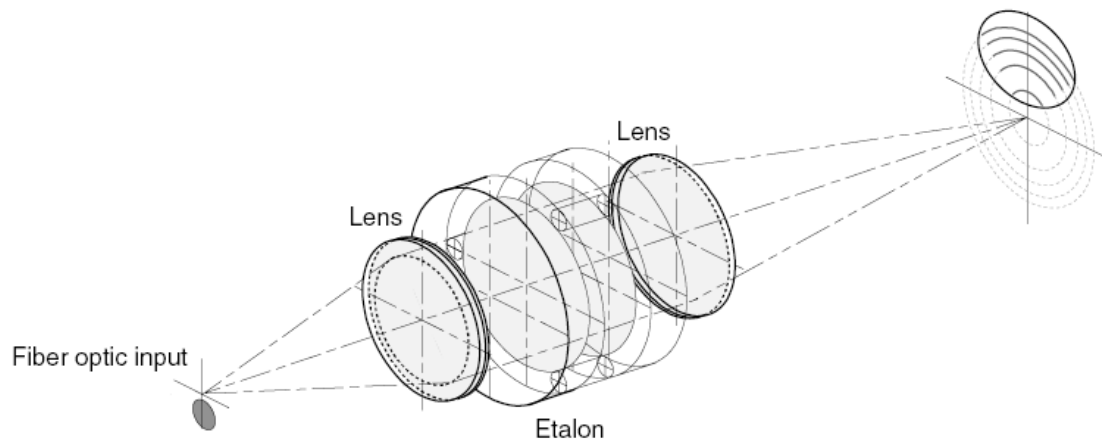
- ❑ For the fringe-imaging technique, by its nature, a multi-element imaging detector is required. Further, the detector has to be capable of being used in a **time-gated mode**, in order to provide the essential range-resolved sampling of the backscattered signal. There is the further subtle difficulty that the Fabry-Perot etalon presents its spectral information as concentric circular fringes.
- ❑ **3-D detection: spatial distribution, altitude range, and time**
- ❑ Multi-channel detectors like an imaging photomultiplier tube (IPD), incorporating a 24-channel concentric-ring anode read-out designed to match the fringe pattern presented by the F-P etalon. It uses a stack of microchannel plates to achieve high electronic gain. Each of 24-channel is time-gated to achieve range-resolved data.
- ❑ Circle-to-Line Imaging Optics (CLIO) can be used to convert the circular fringes formed by a F-P etalon into a linear pattern of spots. Then a conventional linear array detector, such as a CCD, can be used to read the linear fringe pattern.
- ❑ CCD response is slower than PMT and PD, problem in range resolution.

# Circle-to-Line Imaging Optics (CLIO)



# Improving Fringe-Imaging Efficiency

- ❑ When F-P etalon is used, only a portion of the incident light is transmitted through the interferometer, and majority of the incident light is reflected out. Three methods to improve this situation -
- ❑ **Fractional Fringe Illumination:** the etalon is illuminated by a solid angle corresponding to only a fraction of the full FSR, which can result in a significantly higher fraction of the signal being transmitted by the etalon.
- ❑ **Interferometer Photon Recycling:** reflected photons are collected by fibers and then re-illuminate the etalon.
- ❑ **Channel Photon Recycling:** aerosol channel and molecular channel for improvement of wind measurements.



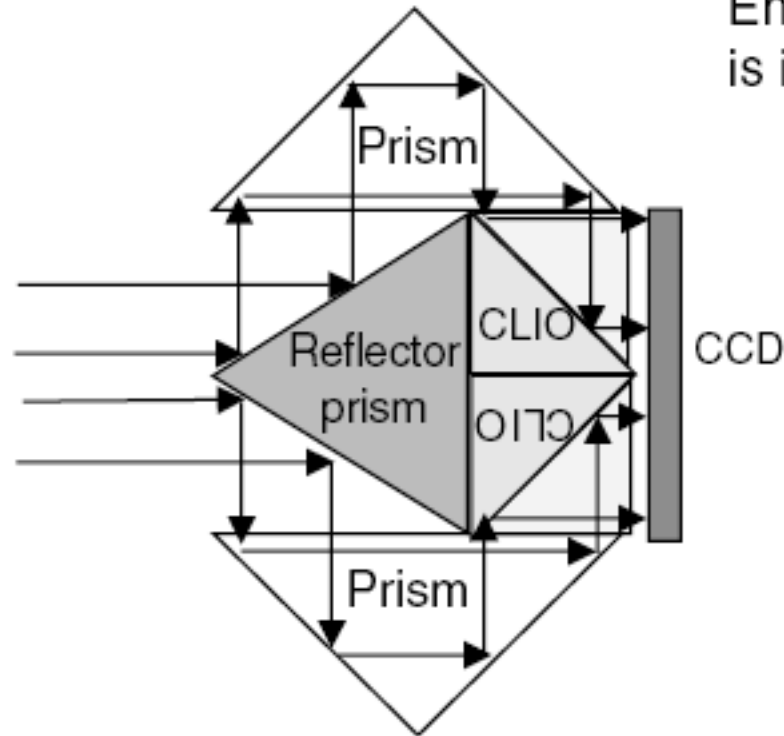


# Photon Recycling + CLIO

End view of input



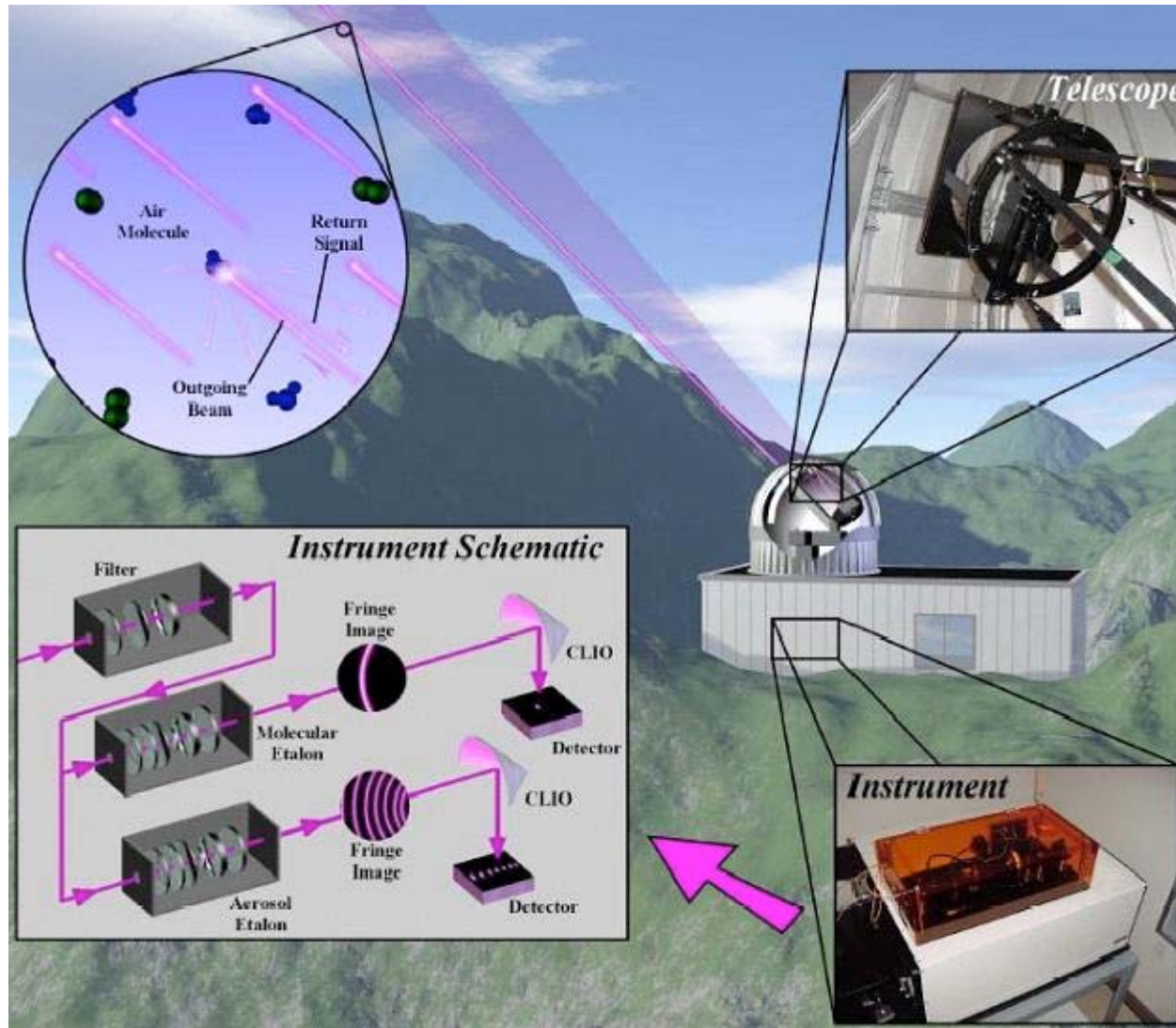
Dual CLIO



End view of what is incident on CCD

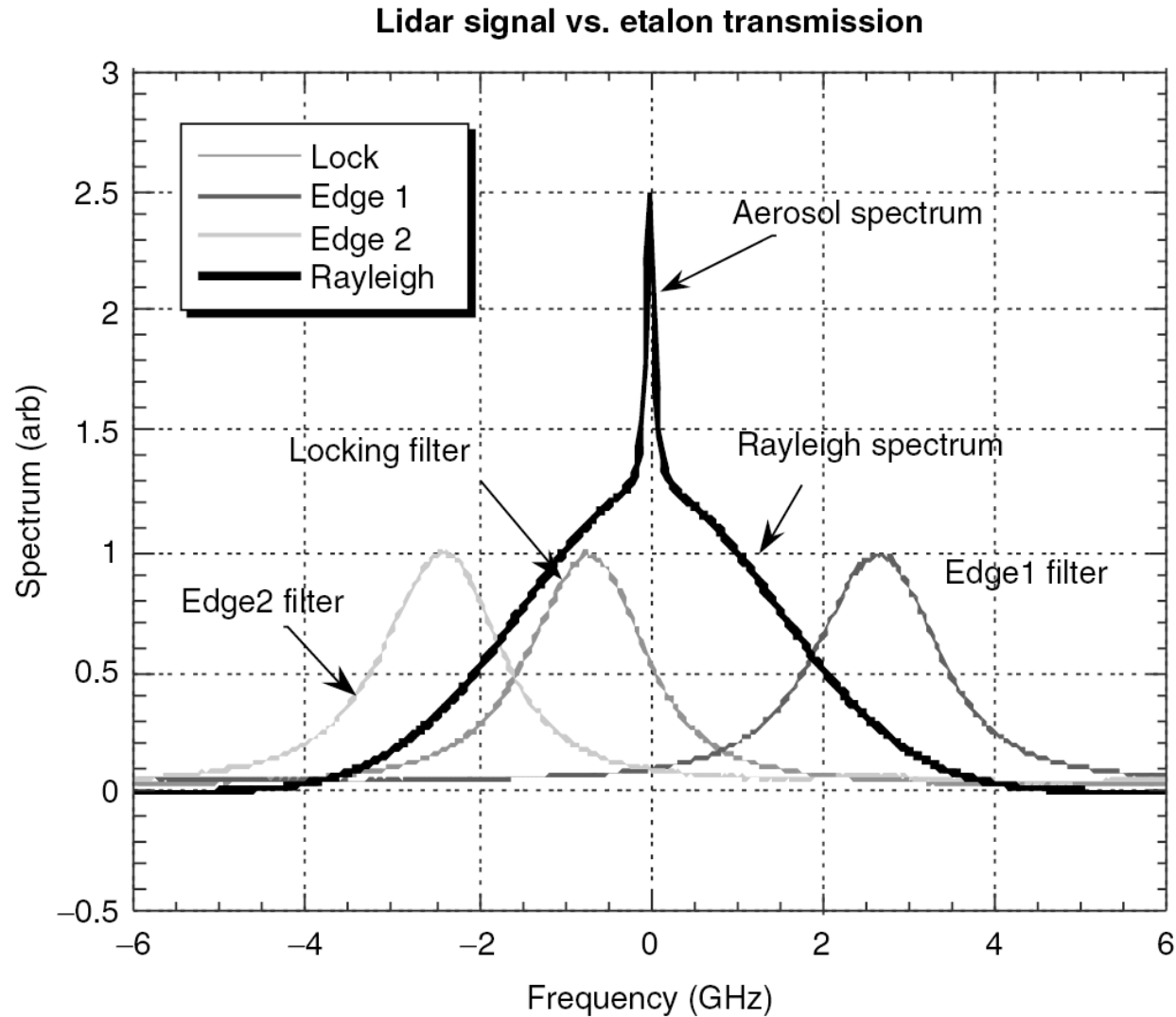


# Example DDL: GroundWinds



<http://groundwinds.sr.unh.edu/>

# Scanning FPI and Edge Filters



The locking filter channel is to ensure the optimum balance of the Edge 1 and Edge 2 filters (F-P etalons) on the zero Doppler-shifted laser signal.

# Freq Analyzer: Single-Edge Filter

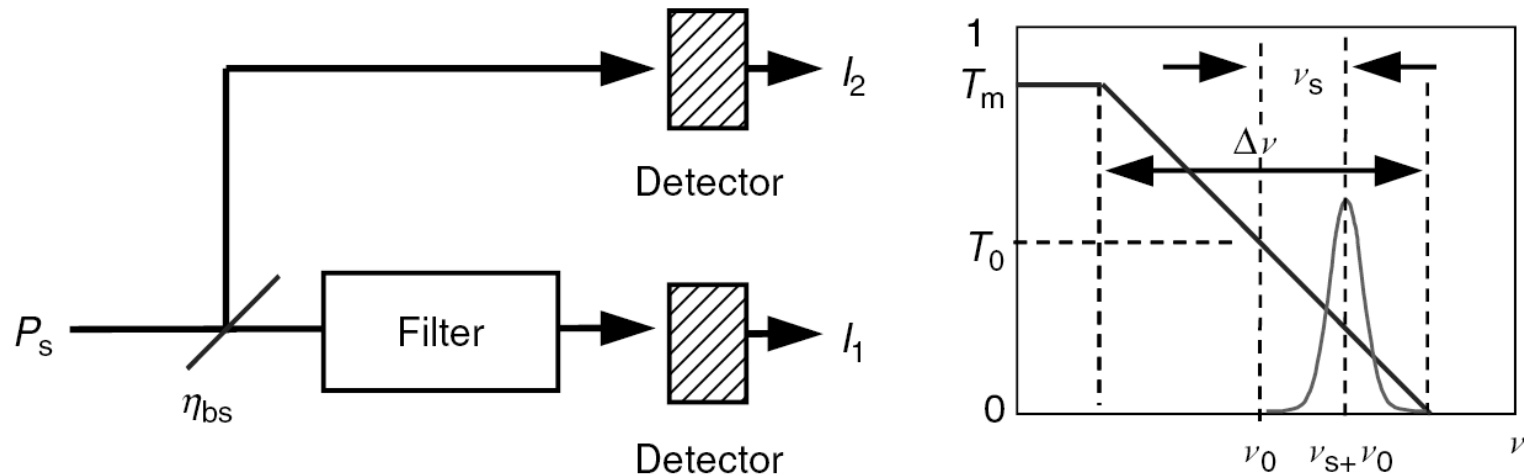


**Figure 7.31** Single-edge functional diagram and filter transmission.

□ A Fabry-Perot etalon or a molecular absorption line is usually employed as the edge filter. The etalon is locked to the zero-Doppler laser frequency,  $\nu_0$ , such that the frequency of the transmitted laser is matched to the mid-point of the quasi-linear transmission edge of the etalon.

□ The intensity ratio of these two channels is a function of the Doppler frequency shift  $\nu_s$ .

$$\begin{aligned}
 S = I_1/I_2 &= \frac{\eta_{bs}}{(1 - \eta_{bs})} \frac{\mathfrak{R}_1}{\mathfrak{R}_2} T_s \\
 &= \frac{\eta_{bs}}{(1 - \eta_{bs})} \frac{\mathfrak{R}_1}{\mathfrak{R}_2} (T_0 - T_m \nu_s / \Delta \nu)
 \end{aligned}$$

# Freq Analyzer: Double-Edge Filter

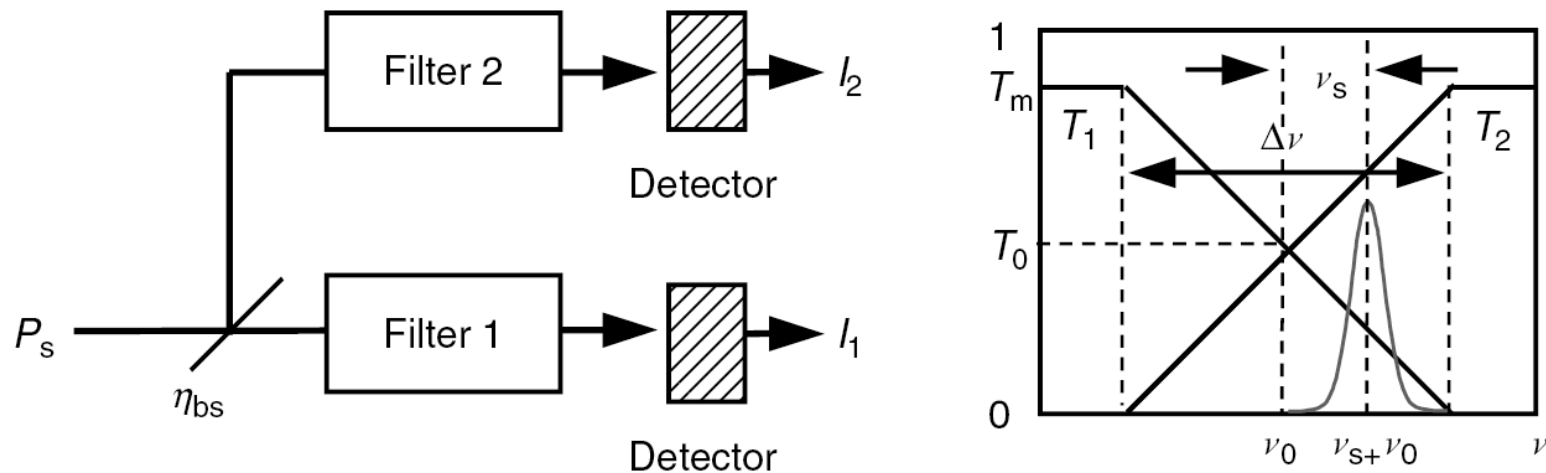


**Figure 7.32** Double-edge functional diagram and filter transmission.

□ Two oppositely sloped quasi-linear discriminator edges are used for the two receiver channels in the double-edge design. Usually etalon transmission fringes are used to create the edges. The etalons are locked together (mid-point) to the zero-Doppler transmitted laser frequency  $\nu_0$ .

□ The intensity ratio of the difference between the two signals to the sum is a sensitive function of the Doppler frequency shift  $\nu_s$ .

$$S = \frac{I_{\Delta}}{I_{\Sigma}} = \frac{I_1 - I_2}{I_1 + I_2} = \frac{T_{s_1} - T_{s_2}}{T_{s_1} + T_{s_2}} = \frac{2\nu_s}{\Delta\nu}$$

# Detectors for FPI Edge-Filter DDL

- ❑ The information presented to the detector in an **edge detection** system is the image of the small on-axis solid angle corresponding to the central on-axis fringe of the Fabry-Perot etalon with the necessary spectral FWHM. A suitable detector will be one that has high quantum efficiency, low noise, the capability for photon counting or analog read-out, depending on the intensity of the signal, and which can be "time-gated" to provide range-resolved information.
- ❑ The conventional PMT, the APD, and the CCD are among several that have been used successfully, depending on the spectral region of the wind lidar. The PMT is a device that is essentially noise-free when used in photon-counting mode. Due to the negligible read-out and electronic noise, the PMT signal may be post-integrated with complete flexibility, leading to the PMT being widely used as a detector of choice, particularly at 355 and 532 nm. Its drawback is the modest quantum efficiency of the photocathode of the device, normally limited to values of order 35% or less, depending on the spectral region.
- ❑ **2-D detection: altitude range and time, similar to other lidars, except the fringe-imaging lidars.**

# Fringe Imaging vs Edge Filters

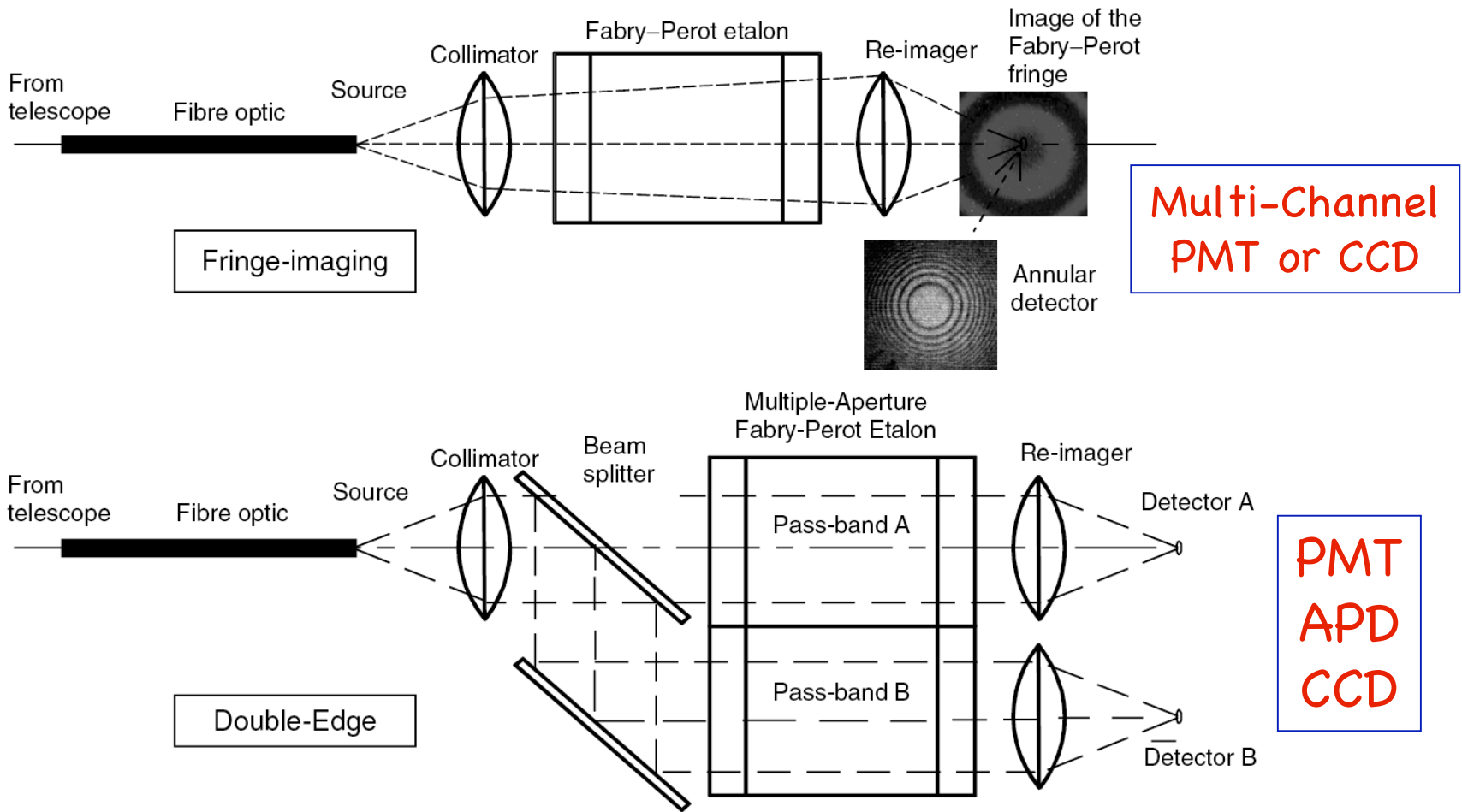


**Figure 7.45** The fringe-imaging and double-edge detection methods for direct detection are shown conceptually.

# Iodine Absorption Lines near 532 nm

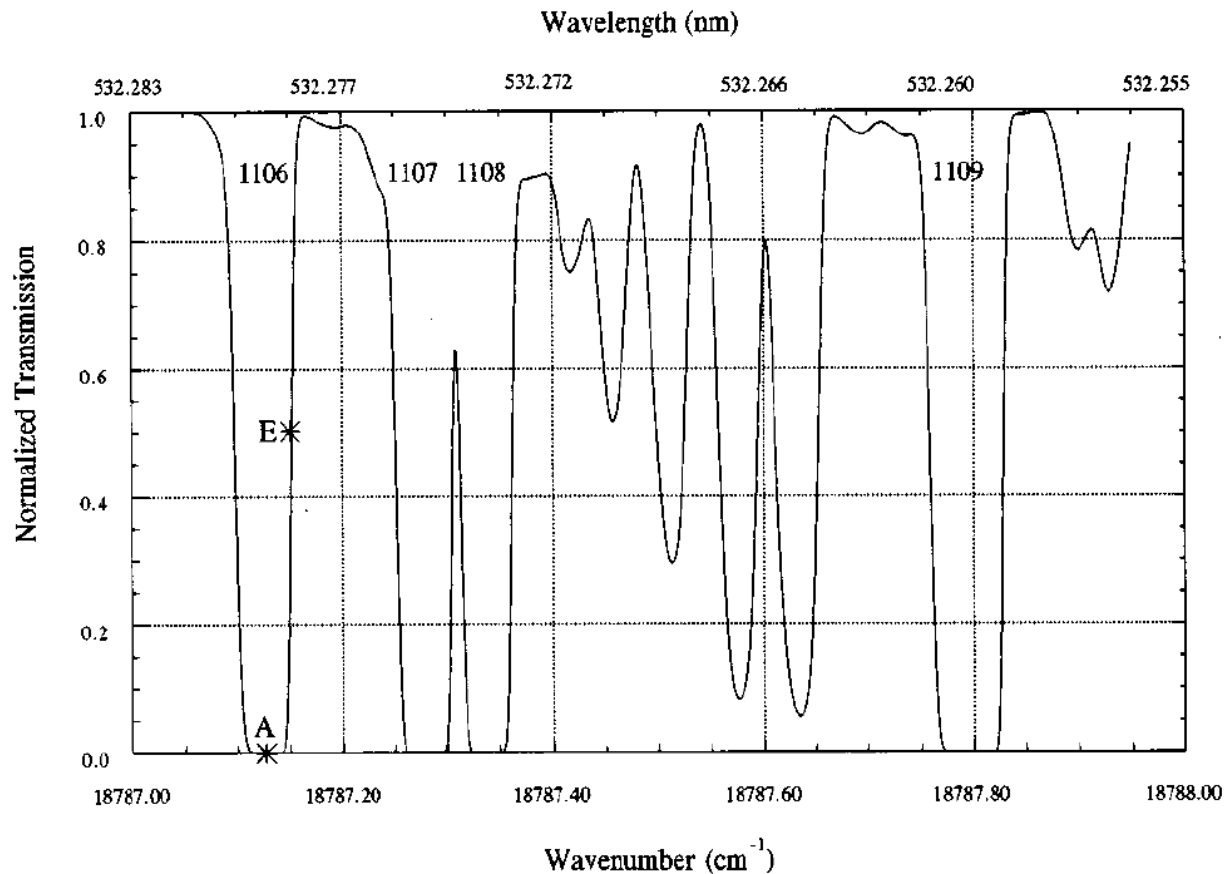


**Fig. 2.** Calculated transmission spectrum near 532 nm of a 10.2 cm long cell with cell and finger temperatures of 60 °C and 55 °C, respectively. The line 1106 shows the two points where the monolithic seed laser can be locked. By locking the laser at both points E and A and making measurements at each frequency, both the Doppler shift and the aerosol mixing ratio can be determined

[Liu et al., Appl. Phys. B 64, 561-566, 1997]



# Iodine Absorption Lines near 532 nm

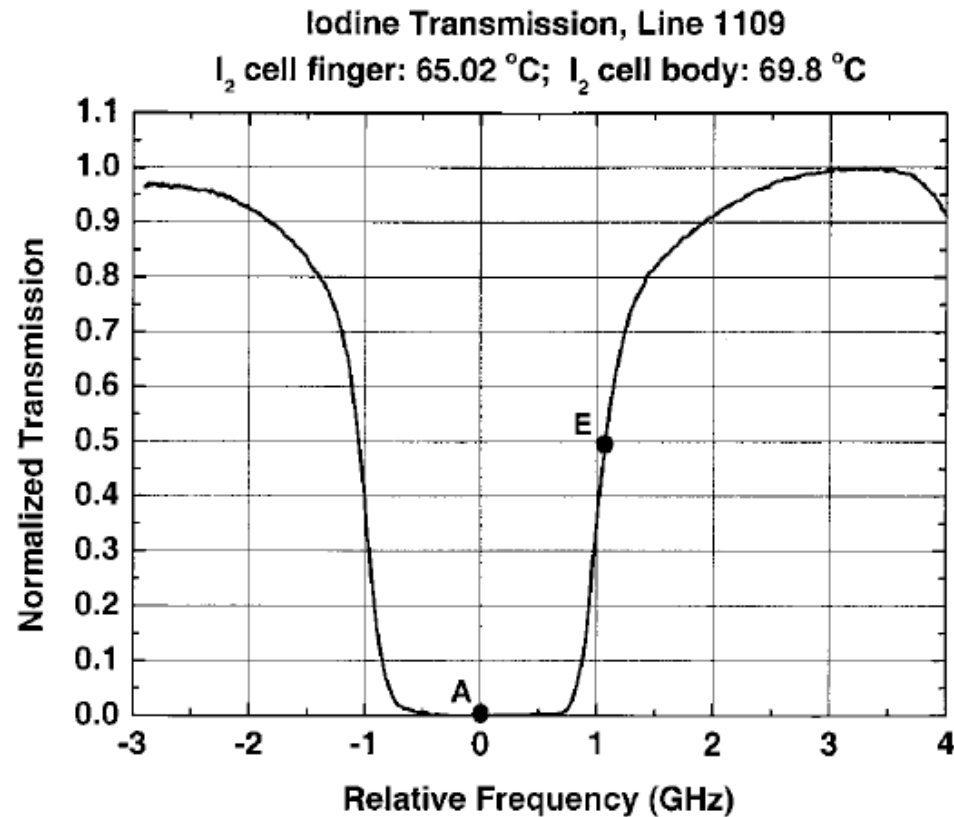


Fig. 2. Normalized transmission for absorption line 1109 of the iodine filter near 532 nm. The temperature of cell finger and cell body are 65.02 °C and 69.8 °C, respectively. The wave numbers at reference point A and locking point E are 18787.796 and 18787.830  $\text{cm}^{-1}$  (1.02 GHz apart), respectively.

[Friedman et al., *Opt. Lett.*, 22, 1648-1650, 1997  
Liu et al., *Appl. Opt.*, 41, 7079-7086, 2002]

# DDL

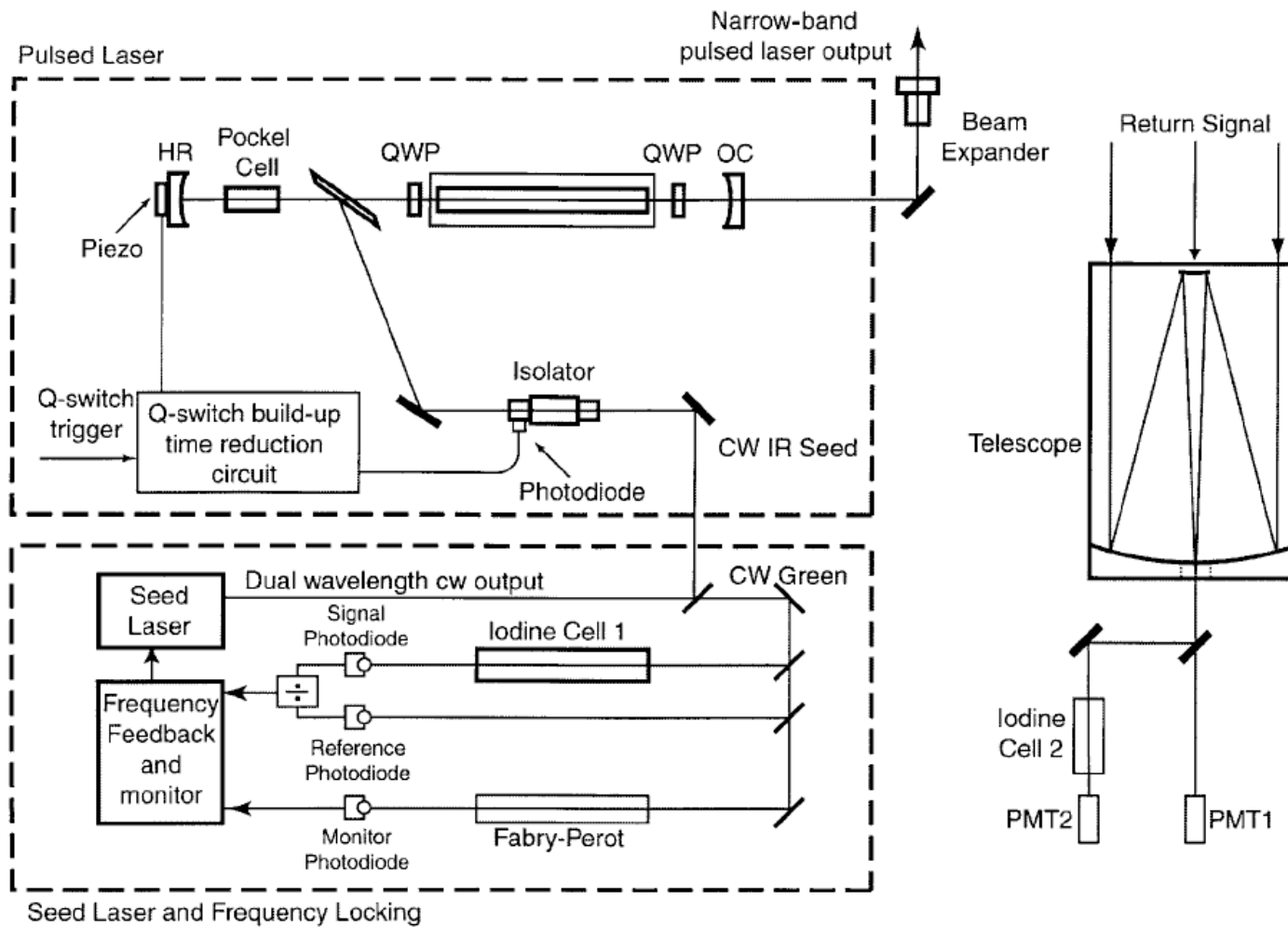


Fig. 1. Schematic diagram for injection-seeded Q-switched pulsed Nd:YAG laser transmitter on the left panels. The lidar receiver is shown on the right, where the iodine cell 2 is the frequency discriminator.

# Iodine Edge Filter DDL

$$N_R = k_R \left( \frac{\Delta r}{r^2} \right) (\beta_a + \beta_m) \exp \left\{ -2 \int dr [\alpha_a(r') + \alpha_m(r')] \right\}, \quad (1a)$$

$$N_M = k_M \left( \frac{\Delta r}{r^2} \right) (f_a \beta_a + f_m \beta_m) \exp \left\{ -2 \int dr [\alpha_a(r') + \alpha_m(r')] \right\}. \quad (1b)$$

$$f_a(\nu) = F(\nu), \quad (2a)$$

$$f_m(T, P, \nu) = \int \mathfrak{R}(\nu' - \nu, T, P) F(\nu') d\nu', \quad (2b)$$

$$\int \mathfrak{R}(\nu' - \nu, T, P) d\nu' = 1, \quad (2c)$$

[Liu et al., Appl. Opt., 41, 7079-7086, 2002]

# DDL

$$R_W(\nu) = \frac{N_M(\nu)}{N_R(\nu)} = \frac{k_M}{k_R} \left[ \frac{f_a(\nu)(\beta_a/\beta_m) + f_m(\nu)}{(\beta_a/\beta_m) + 1} \right], \quad (3a)$$

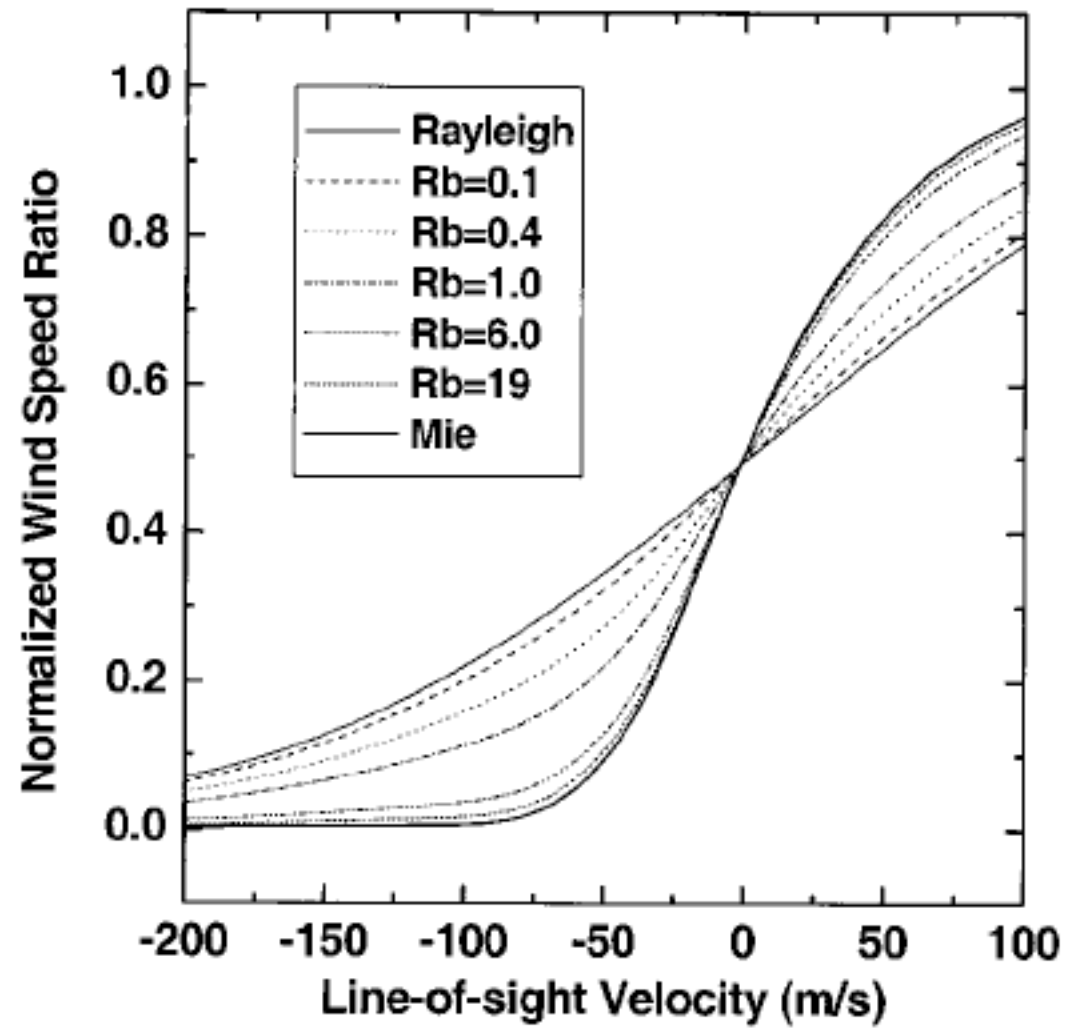
$$R_W(\nu_0) = \frac{N_M(\nu_0)}{N_R(\nu_0)} = \frac{k_M}{k_R} \left[ \frac{f_a(\nu_0)(\beta_a/\beta_m) + f_m(\nu_0)}{(\beta_a/\beta_m) + 1} \right], \quad (3b)$$

$$\text{NWR} = \frac{R_W(\nu)}{2R_W(\nu_0)} = 0.5 \left[ \frac{f_a(\nu)(\beta_a/\beta_m) + f_m(\nu)}{f_a(\nu_0)(\beta_a/\beta_m) + f_m(\nu_0)} \right]. \quad (3c)$$

$$R_b(r) = \frac{\beta_a(r) + \beta_m(r)}{\beta_m(r)} - 1 = \frac{k_M f_m N_R(r)}{k_R N_M(r)} - 1. \quad (4)$$

# DDL

Atmosphere Temperature 238.2K, Altitude ~7km



# Assumptions in Edge-Filter DDL

- ❑ To derive wind from edge-filter DDL, several quantities have to be taken from models or from independent measurements.
- ❑ Temperature profile: since the Doppler broadening (depending on temperature) affects the transmitted signal strength, it has to be pre-determined or taken from models for single or double-edge filters.
- ❑ Aerosol-scattering ratio also has to be determined independently when in the atmosphere region with aerosols. For example, in the I2 filter case, tuning the Nd:YAG laser to point A can eliminate aerosol signal thus deriving the aerosol scattering ratio when combined with the reference channel.
- ❑ Background counts in each channel.
- ❑ Of course, filter transmission functions have to be known and determined to high precision and accuracy.